ELSEVIER

Thermochimica Acta 246 (1994) 249–269

thermochimica acta

Stability-related transitions of amorphous foods

M. Karel [a,*], S. Anglea [a], P. Buera [b], R. Karmas [a], G. Levi [a], Y. Roos [c]

[a] *Department of Food Science, Cook College, P.O. Box 231, Rutgers University, New Brunswick, NJ 08903, USA*

[b] *Comision de Investigaciones Scientificas y Technicas de la Republica Argentina, Buenos Aires, Argentina*

[c] *Department of Food Technology, P.O. Box 27 (Viikki B), FIN 00014, University of Helsinki, Helsinki, Finland*

Received 23 July 1993; accepted 20 April 1994

Abstract

The processing and storage of foods result in changes due to physical processes and chemical reactions. The rates of these changes depend on many factors, but the mobility of the reactants and of other significant food components is often a major factor controlling these rates. Recently, it has been recognized that the glass transitions of food components are important in controlling mobility.

This recognition led to the development of "state diagrams" in which glass transition temperatures (T_g) of major food constituents provide a boundary between regions of low mobility (glasses) and increasing mobility ("rubbers"). This approach has been particularly useful in predicting rates of shrinkage, recrystallization, textural changes and volatile (flavor) loss in carbohydrate-based foods. Work on chemical reactions (non-enzymic browning and lipid oxidation) has also demonstrated the profound effect of glass transitions on the rates of these reactions. The common unifying factor is the effect of glass transition on the diffusivities of important reactants in the materials which undergo the transition.

Keywords: Crystallization; Diffusion; DSC; Glass transition; RMS; Stability

List of symbols

a_w water activity
CAS concentrated amorphous solute

* Corresponding author.

SSDI 0040-6031(94)01868-5

C'_g concentration of maximally freeze-concentrated solution in (mol l^{-1})
C_j constants in Eqs. (5) and (7)
D diffusion coefficient in Eq. (6) in (m^2 s^{-1})
D_0 pre-exponential factor in Eq. (6)
D_g diffusion coefficient at temperature T_g in Eq. (7) in (m^2 s^{-1})
D_T diffusion coefficient at temperature T in Eq. (7) in (m^2 s^{-1})
E activation energy in Eq. (1) in (J g^{-1} K^{-1})
E_D activation energy for diffusion in Eq. (6) in (J g^{-1} K^{-1})
k constant in Eq. (4)
k_B browning rate constant in ([OD] h^{-1})
K_g constant in Eq. (3)
M molecular weight in Daltons
m moisture content in percent
p partial pressure of water in food in Eq. (2) in Pa
p^0 vapor pressure of water at temperature T in Eq. (2) in Pa
Q quality index in Eq. (1)
R gas constant
T temperature in K
T_g glass transition temperature in (°C, K)
T_{g_i} glass transition temperature of pure, anhydrous component compounds in Eq. (4) in K
T'_g glass transition temperature of maximally freeze-concentrated solute in K
T'_{go} onset of glass transition of maximally freeze-concentrated solution
T'_{ge} endpoint of glass transition of maximally freeze-concentrated solution
T_{go} onset of glass transition in K
T_{gm} midpoint of glass transition in K
T_{ge} endpoint of glass transition in K
$T_{(g\infty)}$ limiting T_g at high molecular weight (effective T_g) in Eq. (3) in K
T'_m equilibrium melting temperature of ice in maximally freeze-concentrated solution in K
V specific bulk volume at time t in (ml g^{-1})
V_0 specific bulk volume at time = 0 in (ml g^{-1})
w_i weight fraction of component compounds in Eq. (4)

Greek letters

η viscosity at temperature T in Eq. (5) in (Pa s)
η_g viscosity at temperature T_g in Eq. (5) in (Pa s)
τ_c relaxation time for collapse in h
τ_{Cr} relaxation time for complete crystallization in h
τ_{CRR} relaxation time for propanol release from sucrose in h
τ_{FR} relaxation time for fast release in h
τ_{SR} relaxation time for slow release in h

1. Introduction

The quality of foods depends on a complex set of physical, chemical and biological characteristics. For purposes of studying stability, we make simplifications which allow approximations to the complex reality. These are not perfect but are useful in process design and in choosing storage conditions. One of the simplifications is the assumption that the changes which occur during processing and storage depend on only two parameters: time t and temperature T. Furthermore, it is usually assumed that an index of quality Q may be defined. Then, if the rate of quality changes is zero-order [1–3], the Arrhenius equation may be applied

$$-\frac{dQ}{dt} = ke^{-E/RT} \tag{1}$$

where k is a constant, E is a constant (the so-called activation energy for the process), R is the gas constant, and T is the absolute temperature (K).

In addition to temperature we usually consider the role of water, i.e. the moisture content m and water activity a_w

$$a_w = \left(\frac{p}{p^0}\right)_T \tag{2}$$

where p is the partial pressure of water in the food and p^0 the vapor pressure of water at temperature T.

A "stability map" giving a schematic indication of relative rates of biological, enzymatic and some chemical processes in foods stored at a constant temperature as a function of a_w was presented by Labuza et al. [4]. Versions of this "map" have been published subsequently [5,6]. It was recognized that time-dependence and non-equilibrium conditions require extreme caution in the use of the water activity dependence of reactivity [7,8]. Nevertheless the concept proved useful, in particular in describing two types of changes: those due to microbial growth and those due to non-enzymatic browning. With respect to microbial growth, there are excellent theoretical and empirical reasons to conclude that water activity is the determinant of growth (because it determines the osmotic stress, and because the ability to grow is determined by the degree of that stress, and the osmoregulatory capacity of a particular cell) [9].

2. Glass transitions in foods

It has been proposed that effects of moisture and temperature on the rate of food changes are related to the physical state of the food, and specifically to the temperature above the glass transition temperature T_g. The fact that many foods form amorphous glasses is known and the consequences of glass transitions in food and related systems has been described [10–12]. A systematic analysis of many processes, and the development of a stability map based on the T_g curve in a

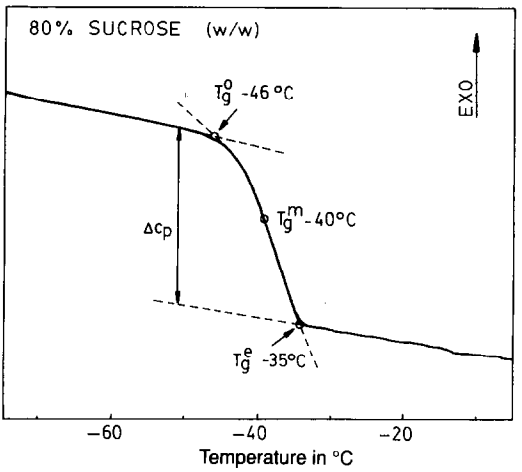

Fig. 1. Glass transition temperature (T_g) range of amorphous sucrose with 20% water. The T_g has its onset at T_{go}, midpoint at T_{gm} and endset at T_{ge}.

temperature–concentration or temperature–water-content plot has been undertaken and reported in a very extensive series of papers by Levine and Slade [13,14]. These reviews have voluminous citations to research papers and other reviews.

The T_g values of food components vary from that of water at −135°C [15,16] to very high temperatures for food polymers such as polysaccharides and proteins [17,18]. The T_g of food components is most often determined by differential scanning calorimetry (DSC) [19–21]. A typical DSC trace of the glass transition ranges of an amorphous sugar is shown in Fig. 1. Recent studies have reported the use of other methods such as mechanical spectrometry [22–24], dynamic mechanical thermal analysis [25], thermal mechanical analysis [26] and nuclear magnetic resonance [25]. T_g values may be reported as onset or midpoint temperatures of the transition range. We prefer the use of onset values as defined in Fig. 1, because many changes in food materials, e.g. the crystallization of amorphous sugars, are initiated when the onset temperature is exceeded [27].

Plasticizers, including water, depress T_g drastically. The typical effect of moisture content m on T_g is shown in Fig. 2. A typical plot of T_g versus a_w is shown in Fig. 3. The T_g values of polymers are related to molecular weight [28,29]

$$T_g = T_{g(\infty)} - K_g M^{-1} \tag{3}$$

where M is molecular weight in D, K_g is a constant, and $T_{g(\infty)}$ is the limiting T_g at a high molecular weight in K.

The T_g values of glucose oligo- and polysaccharides follow Eq. (3) [18]. We have used Eq. (3) to predict the T_g of anhydrous starch as shown in Fig. 4. The T_g values of solutions, and mutually soluble mixtures can be calculated using Eq. (4) [30]. We

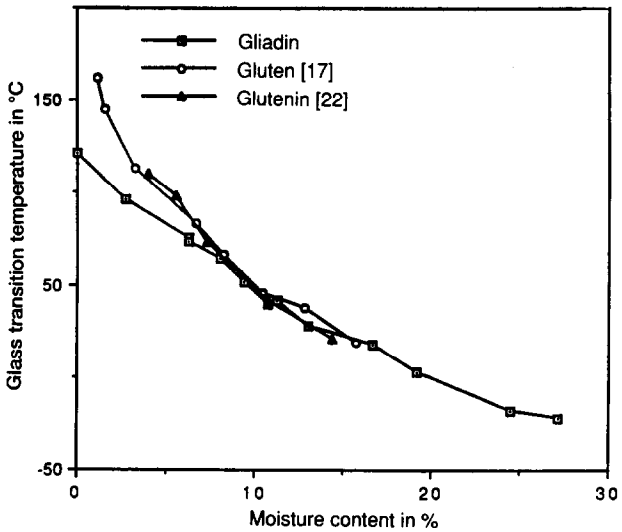

Fig. 2. The glass transition temperature of gliadin, glutenin and gluten as a function of moisture content [17,22,24].

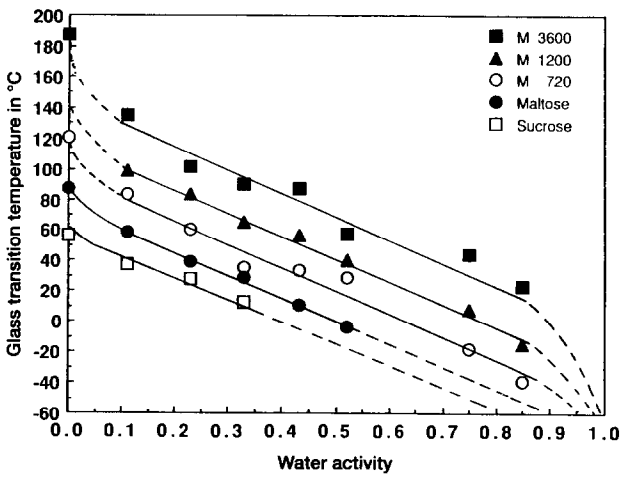

Fig. 3. Effect of water activity of glass transition temperatures of sugars and maltodextrins.

were able to predict the effect of water on the T_g of a wide range of carbohydrate materials [18,23,29,31]

$$T_g = \frac{w_1 T_{g_1} + k w_2 T_{g_2}}{w_1 + k w_2} \tag{4}$$

where w_i are the weight fractions of component compounds, T_{g_i} are the glass transition temperatures of the anhydrous pure component compounds in K, and k is a constant.

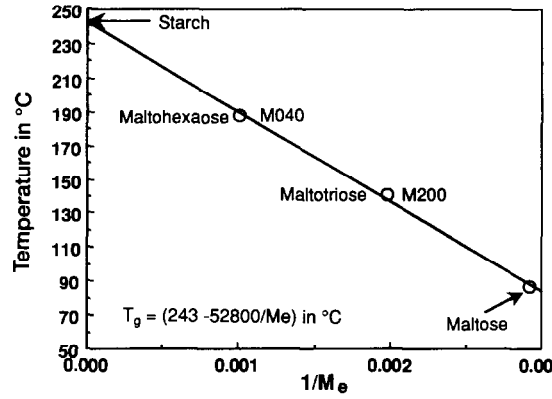

Fig. 4. Effect of molecular weight on the glass transition temperature (T_g) of glucose polymers and maltodextrins. $1/M_e$ (effective molecular weight) predicts the T_g of anhydrous starch to be at 243°C.

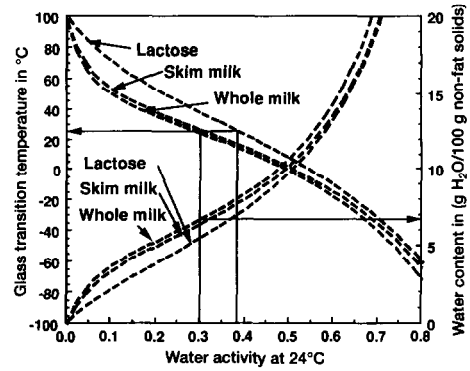

Fig. 5. Glass transition temperature (T_g) and equilibrium water content at 24°C as a function of water activity of lactose, skim milk and whole milk. The critical water activity range and water content assume that stability decreases as the T_g decreases below ambient temperature.

A combined use of Eq. (4) and water sorption isotherms [32] allows evaluation of T_g at various storage conditions. Diagrams showing both equilibrium water content and T_g as a function of water activity (Fig. 5) can also be used to determine critical values of a_w and m, above which the stability at ambient temperature is likely to decrease because T_g is depressed below that temperature. Most foods have high water contents and their theoretical T_g values are close to that of pure water. However, ice formation occurs below the freezing point. As the ice formation proceeds, the equilibrium freezing point of water decreases due to solute concentration in the unfrozen phase. A maximally freeze-concentrated unfrozen solution is formed in a relatively narrow temperature range between the T_g of the maximally freeze-concentrated solute (T'_g) and the lowest equilibrium melting point of ice within the unfrozen matrix (T'_m) [33]. Both T'_g and T'_m have values that are independent of the initial solute concentration (Fig. 6).

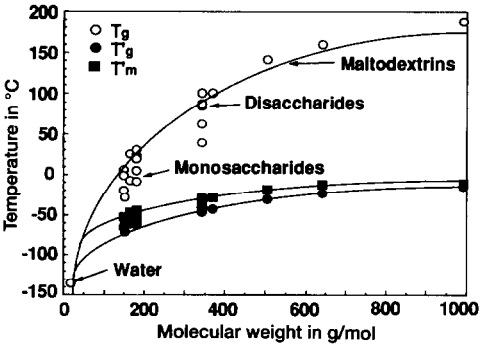

Fig. 6. Glass transition (T_g), glass transition of the maximally freeze-concentrated solute (T'_g), and onset temperatures of ice melting within the maximally freeze-concentrated solute (T'_m) of various carbohydrates as a function of their molecular weight.

The solute concentration of the maximally freeze-concentrated unfrozen matrix C'_g can be calculated with Eq. (4). Recent studies show that solute concentrations in maximally freeze-concentrated carbohydrate matrices are approximately 80% [31]. Because of kinetic constraints, solutions with high initial solute concentrations (60–80%) may require several days or even weeks of annealing at $T'_g < T < T'_m$ until the maximally freeze-concentrated state is achieved. Both T'_g and T'_m depend on the molecular weight of the solute. Roos and Karel [18] reported that above a certain molecular weight T'_g and T'_m have the same value (Fig. 6). Experimental T_g, T'_g, C'_g and T'_m data for most common sugars were recently reported by Roos [31].

The T_g, T'_g, and T'_m data of food materials can be plotted as a function of water content. Such state diagrams were originally proposed by Franks et al. [34]. State diagrams are important in the characterization of the physical behavior of food materials under various processing or storage conditions [35]. A typical state diagram shows the T_g line as a function of concentration with T'_g and T'_m values (Fig. 7). The temperature-dependence of viscosity is often found to be given by Eq. (5) and can be included in state diagrams to show isoviscosity states above T_g. Such isoviscosity lines can be used to evaluate rates of dynamic phenomena above T_g

$$\log \frac{\eta}{\eta_g} = \frac{C_1(T - T_g)}{C_2 + (T - T_g)} \tag{5}$$

where η is viscosity at temperature T in (Pa s), η_g is viscosity at $T = T_g$ in (Pa s), and C_1 and C_2 are constants.

Williams et al. [36] found average coefficients applicable to mechanical relaxation in polymers to be: $C_1 = -17.44$ and $C_2 = 51.6$. Soesanto and Williams [37] found these coefficients valid for the WLF correlation of the viscosity of sugars.

3. Dependence of physical changes on transitions: stickiness and caking

Stickiness and caking may cause problems in production and storage of dehydrated food powders [12,38]. Stickiness has been observed to occur at a "sticky

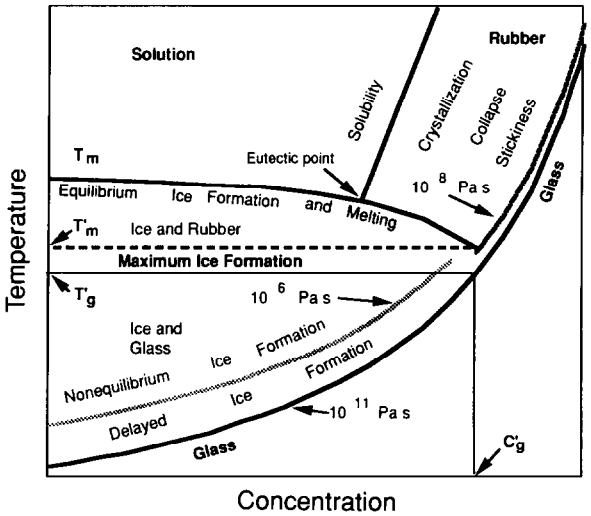

Fig. 7. State diagram showing the glass transition temperature (T_g) and changes in material physical state above T_g. The state diagram may be used to evaluate equilibrium and non-equilibrium phenomena at various water contents and temperatures.

point" temperature defined by Lazar et al. [38] as the temperature at which the force required to stir a food powder increased sharply. Downton et al. [39] reported that stickiness occurs as the viscosity of the powder decreases below 10^7 Pa s. Because the viscosity of amorphous food powders decreases rapidly above T_g, stickiness may also be related to the temperature difference between ambient temperature (T) and T_g [35]. We have demonstrated that the critical viscosity for stickiness as reported by Downton et al. [39] is equivalent to the viscosity of amorphous sugars at ($T - T_g$) values of 10–20°C; stickiness may, however, occur at lower ($T - T_g$) values when food is exposed to temperatures above T_g for long times. Isoviscosity lines in state diagrams can be used to show critical viscosities for stickiness and the time needed to a given degree of collapse, which may be used as a quantitative prediction of stability (Fig. 7). Structural changes above T_g result from a decrease in viscosity and resultant flow, because the liquid-like material above T_g has a tendency to minimize its volume. Stickiness and caking temperatures are also needed in the design of agglomeration processes, which use controlled stickiness to control particle sizes of food powders.

4. Crystallization

Water sorption isotherms of many food powders show loss of adsorbed water above a characteristic water activity, due to sugar crystallization. Makower and Dye [40] showed that crystallization of amorphous sucrose and glucose proceeds at a rate dependent on water content, and many studies have confirmed that sugars in

amorphous powders may crystallize during water adsorption or heating [12,27]. Rapid crystallization may be observed by isothermal DSC at an approximately constant $(T - T_g)$ value independent of moisture content [27]. The rate of crystallization depends on viscosity and the relationship between $(T - T_g)$ and time to a given extent of crystallization was correlated using the WLF equation (Eq. (5)). We have also shown that the rate of crystallization is accelerated in hermetically sealed containers [41] due to increasing plasticization by water released from the crystallized material. Crystallization affects food stability by releasing encapsulated materials such as lipids, which subsequently show increasing rates of oxidation [42]. Retrogradation of starch during bread staling has also been related to crystallization of amorphous amylopectin [43].

5. Non-equilibrium ice formation

Most foods contain solutes which do not crystallize readily from freeze-concentrated solutions. In such solutions the unfrozen mixture of solute and unfrozen water may become glassy. Ice formation is affected by various factors including the initial water content, temperature and time. Rapid cooling of solutions may result in non-equilibrium ice formation, partial freeze-concentration, and ice formation during rewarming (devitrification) (Fig. 8). Devitrification is observed as an exothermal transition, which results from the release of latent heat from ice

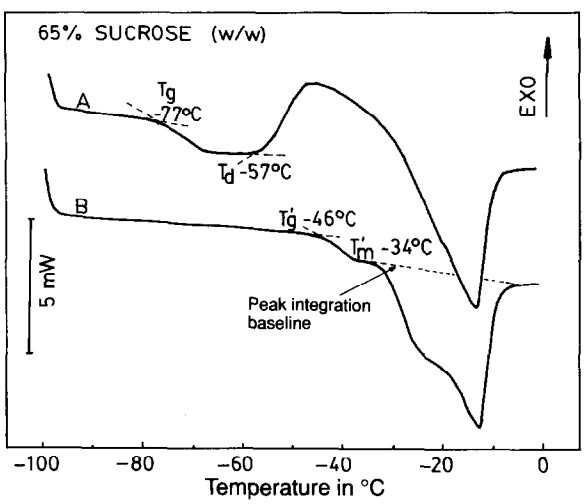

Fig. 8. Thermal behavior of a frozen sucrose solution. (Initial sucrose concentration = 65%.) Rapid cooling results in partial freeze-concentration (A), which can be observed from a low glass transition temperature (T_g) and devitrification (T_d) during rewarming. Maximum freeze-concentration can be achieved by annealing the solution at −35°C (below onset of ice melting, T'_m). The thermogram of the annealed solution (B) shows the glass transition temperature of the maximally freeze-concentrated solution (T'_g) and ice melting at T'_m.

formation. The devitrification temperature T_d increases with increasing rewarming rate, indicating that ice formation above a preceding T_g is time-dependent [23,29]. The increasing amount of ice decreases water content and increases the T_g of the unfrozen matrix. The increased T_g value decreases the rate of ice formation as the $(T - T_g)$ decreases, resulting in increasing viscosity [23,29]. We have shown that isothermal annealing above T_g can be used to form ice in carbohydrate solutions and proposed that the rate of ice formation is determined by $(T - T_g)$ [23,29]. Melting of ice in maximally freeze-concentrated solutions starts at a temperature characteristic for a given material [23,29,31]. Above this temperature (T'_m), eutectic crystallization of sugars may also occur as the amount of unfrozen water increases and viscosity decreases (Fig. 7). A typical example of such behavior is lactose crystallization in ice cream, which can be delayed by adding polysaccharides to increase the viscosity of the unfrozen phase.

6. Collapse of pores during drying

Structural collapse (defined as a decrease in specific volume) during drying affects product quality by reducing porosity, rehydration ability and texture. We have studied these structural changes during freeze drying below and above T_g. In freeze drying, sublimation of ice creates pores, the walls of which may collapse due to surface forces or gravity. The high viscosity of the concentrated amorphous solution (CAS) [44], a major component of pore walls, prevents or retards collapse. The premise of our work was that if the temperature of the CAS remained below T_g during drying, no collapse would occur because the viscosity would be very high (approximately 10^{11} Pa s) [45]. Collapse during freeze drying has been related to the collapse temperature, which is close to but higher than T_g [46]. Increased plasticization of the CAS by unfrozen water occurs above the temperature at which the ice begins to melt (T'_m), decreasing the viscosity and causing acceleration of collapse. Resonance mechanical spectrometry (RMS) and differential scanning calorimetry (DSC) were used to determine the T_g of potato, apple and celery. Fresh plant tissues were found, by both methods, to have a T_g of approximately $-46°C$. It was assumed that during freezing they were concentrated to the same extent. We detected an apparent crystallization of some unfrozen water during thermal analysis and in RMS studies; thus it appears that maximum freeze-concentration did not occur. The T_g determined by mechanical spectrometry is known to correspond to the "endset" of the transition measured by DSC [22,47]. The onset glass transition temperature of a maximally concentrated amorphous sucrose solution (T'_{go}) has been shown by Roos and Karel [33] to be $-46°C$ and the endpoint (T_{ge}) to be $-35°C$. Comparing T_{ge} determined by DSC with T_g estimated by RMS shows some differences. Nevertheless we could estimate the T_g of our experimental samples to be in the vicinity of the T'_{go} ($-46°C$). Freeze drying was performed under high vacuum (0.53 Pa) and reduced vacuum conditions (90.64 Pa and 209.28 Pa) to obtain varying initial sample temperatures that were below ($-55°C$), near ($-45°C$) and above ($-28°C$) the T_g of these materials. Collapse was determined by

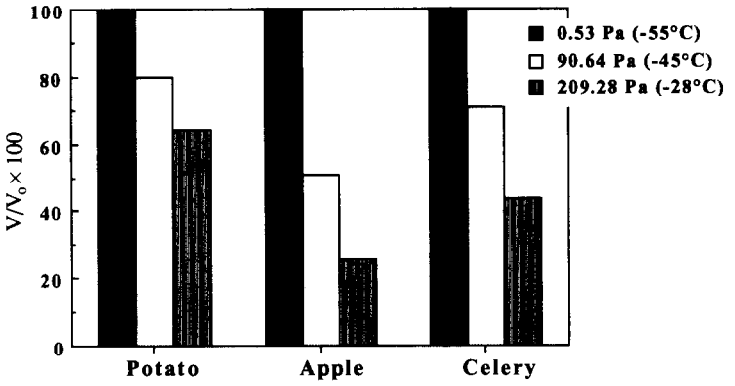

Fig. 9. Collapse (measured as volumetric shrinkage) during freeze drying of potato, apple and celery.

measuring the bulk volume before and after freeze drying, expressing the change as $(V/V_0) \times 100$, where V is the bulk volume at the end of drying and V_0 is the initial bulk volume. Fig. 9 shows the collapse of apple, potato, and celery during freeze drying. T'_m, the onset of melting, was approximately $-32°C$ [48] in these plant tissues. Because of ice melting, detrimental effects in the $-28°C$ sample occurred due to both the glass-to-rubber transition and melting which freed water to plasticize the matrix. Apple and celery showed more collapse than fresh potato due to the initial higher volume of water in apple and celery. Fresh potato contains 3.72 g H_2O/g solids compared to 7.9 and 18.96 g H_2O/g solids for apple and celery, respectively. The temperature T'_m, above T_g, can result in substantial collapse, thus emphasizing the importance of the glass transition in structural changes during drying.

7. Diffusional processes as affected by phase transitions

Many changes in foods (reactions, flavor loss) are affected by the diffusivity of the components. Two approaches have been widely used to express the dependence of diffusivity in amorphous materials. The first considers temperature dependence to be given by the Arrhenius equation, but with the activation energy E_D being different above and below T_g [48]

$$D - D_0 e^{-E_D/RT} \tag{6}$$

where D is the diffusivity at temperature T ($m^2\ s^{-1}$), D_0 the pre-exponential factor, E_D the activation energy for diffusion (J g^{-1} K^{-1}), R the gas constant, and T absolute temperature (K).

The difference between the activation energies below and above T_g depends on diffusant size and on the packing density of the amorphous matrix. A typical plot resulting from the above assumption is shown in Fig. 10. The second approach relates the diffusivity to viscosity above T_g assuming a reciprocal relationship

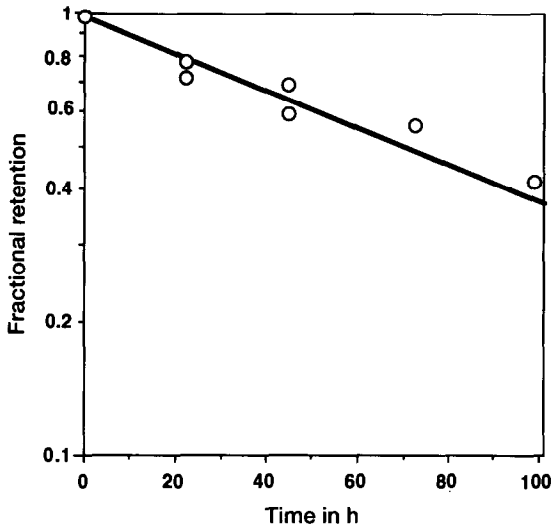

Fig. 10. Initial release of *n*-propanol from anhydrous sucrose:raffinose (3:2) as a function of time in a matrix maintained at $(T - T_g) = 15°C$. Release is linear when plotted on a semi-log axis showing exponential behavior.

between D and viscosity (η). It has been suggested [13] that this dependence can be expressed by a modification of the WLF equation [36], assuming that D is inversely proportional to η

$$\log \frac{D_g}{D_T} = \frac{C_1(T - T_g)}{C_2 + (T - T_g)} \tag{7}$$

where D_T is the diffusivity at temperature T (K), D_g is the diffusivity at reference temperature T_g (K), C_1 and C_2 are constants, and T_g is the glass transition temperature (K).

An important application in food technology is the controlled release of entrapped food components or additives. It is feasible to incorporate such entrapped volatile components (as particles, droplets, or individual molecules) in glasses formed by other food components, e.g. sugars, by drying, extrusion or other methods [49]. Their release may be controlled by achieving specified $(T - T_g)$ levels. A drastic decrease in retention of volatiles in carbohydrate glasses above a "collapse temperature" (T_c) has in fact been observed and attributed to T_c being above T_g [50,51]. In most systems, glass transition also allows deformation under gravitational forces and collapse due to the elimination of pores and cavities [45,51,52]. The resulting increase in bulk density may also affect diffusion. Water, which acts as a plasticizer in carbohydrate systems [13,18], lowers T_g and accelerates flow processes [54,55]. The relationship between the relaxation time for various processes, including "collapse", and the temperature above T_g has been shown to be given in many cases by the WLF equation. Because, in practice, in many cases collapse processes coincide with the release of part of the entrapped materials, we

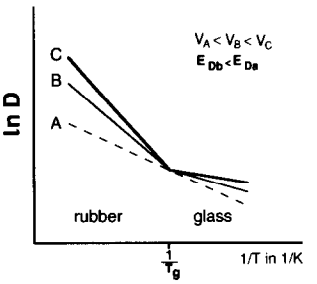

Fig. 11. Arrhenius plot of the effect of temperature on the diffusivity of helium (A), methanol (B) and ethyl bromide (C) in poly(vinylacetate) above and below T_g. The larger the penetrant, the larger the difference in activation energy for diffusion (E_D) below and above T_g, where E_D above T_g is greater than E_D below T_g. (See Ref. [48].)

have carried out studies in model systems to analyze the dynamics of both processes. Amorphous sugar glasses were prepared by freeze-drying of 25% (w/w) sugar solutions. The diffusant entrapped within these glasses was radio-labelled *n*-propanol. Sucrose solutions gave a system which crystallizes readily above T_g, and sucrose:raffinose (3:2) mixture, a system in which crystallization was inhibited. We noted that the initial release of the entrapped volatiles from the sucrose:raffinose matrices was exponential (Fig. 11). The exponential release allows the calculation of a relaxation time for release. The collapse as measured by volumetric shrinkage is also exponential, and τ_c (relaxation time for collapse) can be calculated. The release of a portion of the enrapped volatiles during collapse was designated as fast release, with the relaxation time being τ_{FR}. In sucrose system, crystallization coincides with the complete release of entrapped propanol. Relaxation times for both collapse and the initial fast release (τ_c, τ_{FR}) were found to be dependent on $(T - T_g)$ and the WLF equation was used to correlate this dependence. Complete crystallization of sucrose above T_g was also found to be exponential with relaxation time τ_{Cr}. The WLF correlation of relaxation times for propanol release in the sucrose system (τ_{CRR}) and of the time required to achieve complete crystallization (τ_{Cr}) are shown in Fig. 12. Because crystallization leads to complete release of propanol and the release kinetics are of the first-order type, it is not surprising to see that both relaxation times are of similar magnitude. The WLF equation with the original constants (-17.44 and 51.6 for C_1 and C_2 respectively) gives a good prediction of the dependence of τ_{Cr} and τ_{CRR} on the temperature above T_g. In systems with inhibited crystallization, rapid release occurs, followed by a much slower release of the remaining propanol (Fig. 13). We found that the slow release can also be analyzed, assuming exponential release, and a relaxation time (τ_{SR}) calculated. The observations may be explained by assuming that freeze drying results in a porous system, with the diffusant entrapped in the walls of the pores (Fig. 14A and B). The softening of the walls results in pore collapse. Part of the propanol is released during this process ("fast" release step) (Fig. 14C). Once the collapse is complete, the release of the portion of the propanol remaining within the matrix occurs by diffusion through a dense matrix (Fig. 14D). A schematic diagram

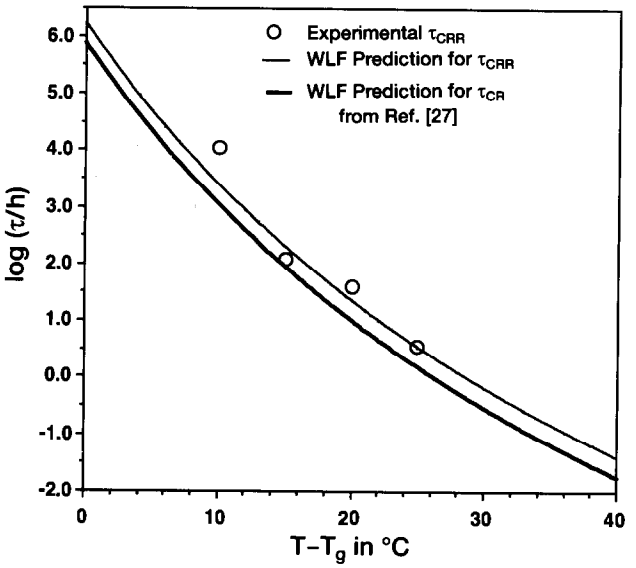

Fig. 12. Effect of $(T - T_g)$ on the relaxation time for complete crystallization of anhydrous sucrose (τ_{Cr}) and *n*-propanol release (τ_{CRR}). Solid lines represent the WLF equation for each pair of τ and $(T - T_g)$, averaging over the full range of data pairs.

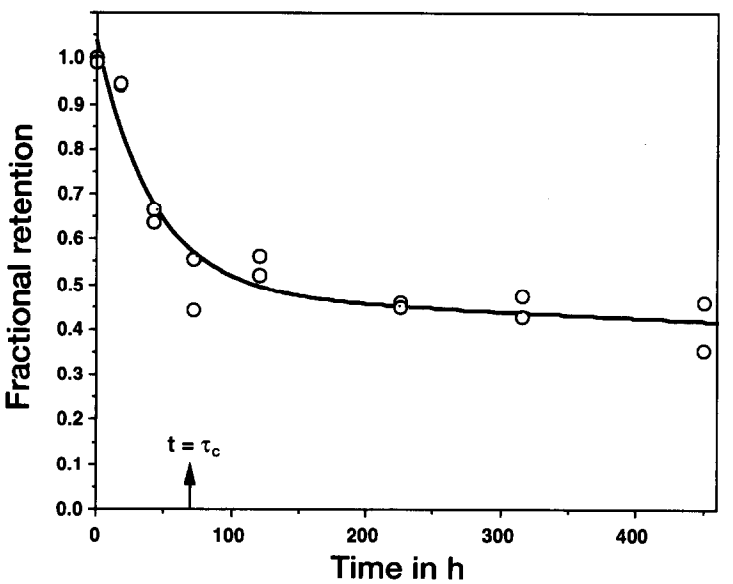

Fig. 13. *n*-Propanol release from sucrose:raffinose (3:2) matrix at $(T - T_g) = 15$°C and 2% moisture, as a function of time. After the initial "fast" release coinciding with matrix flow, a considerable decrease in release rate is observed at $t > \tau_c$, indicated on the time axis ($\tau_c = 72$ h).

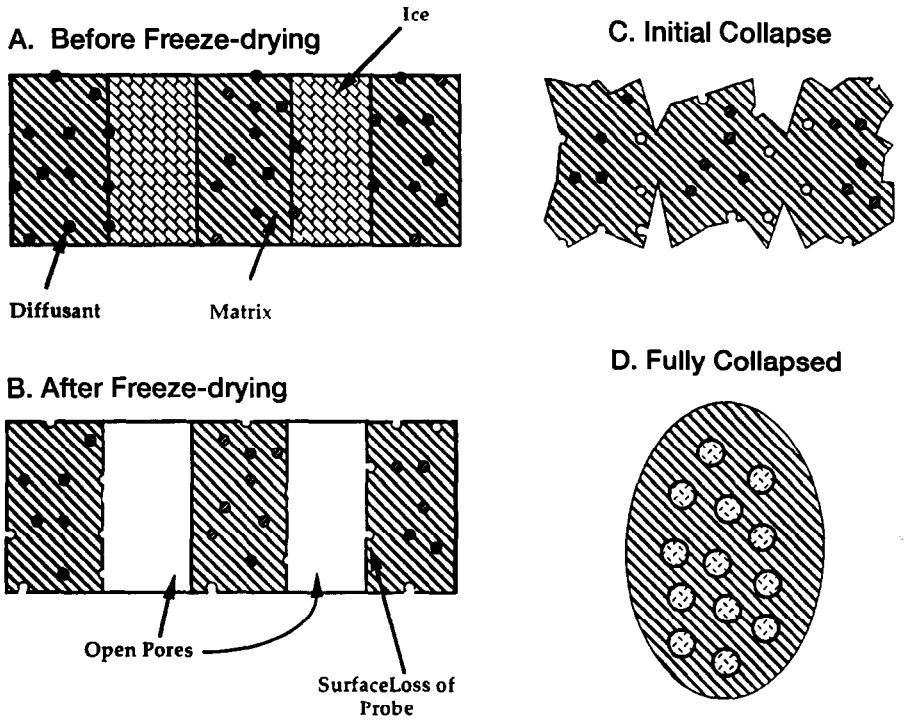

Fig. 14. Schematic diagram of the encapsulation of organic compounds during freeze-drying. A. After freezing, before drying, the crystallizing ice excludes any soluble and insoluble compounds thus concentrating it and, with the rapid increase in viscosity, forming concentrated amorphous solute (CAS) containing both the matrix and the organic compounds. B. After drying ($T < T_g$). Ice sublimation results in pores and the formation of glass with the entrapped compounds. Compounds in contact with the pores will be lost. C. After drying ($T > T_g$), $t < \tau_c$. Initial pore collapse and matrix flow results in exclusion of part of the entrapped compounds to the pores or the surface where they will be lost ("fast" release). D. After drying, $T > T_g$, $t > \tau_c$. Pores are gone, the matrix is collapsed and probe release is mainly due to diffusional process in the dense "rubbery" matrix.

describing the release from crystallizing and non-crystallizing systems is shown in Fig. 15. The relaxation times for these processes were obtained experimentally and are shown in Table 1.

8. Effect of glass transition on rates of chemical reactions

It has been suggested that glass transitions may result in increased mobility of reactants, because reactions may be diffusion-limited below T_g as summarized in Fig. 16 [53]. However, the increased diffusivity above T_g removes this limitation. Diffusion limitations have in fact been proposed as the cause of lower rates of non-enzymatic browning (NEB) at low moisture contents. We have studied the effect of glass transition on browning of a reactant mixture of an amino acid and

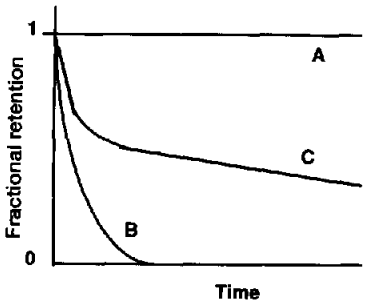

Fig. 15. Schematic representation of release of probe entrapped within amorphous, initially porous, matrices in consequence of exceeding the glass transition temperature, as a function of time. A. Below T_g, no crystallization, collapse or release will occur within a reasonable time frame. B. In a crystallizing system, probe release will follow crystallization. C. In a non-crystallizing system, initial fast partial release coincides with collapse, followed by slower release in the collapsed system.

Table 1
Relaxation times for propanol release in sucrose:raffinose above T_g

$(T - T_g)$ in °C	Anhydrous, $T_g = 63$°C			$m = 2$, $T_g = 52.5$°C		
	τ_c	τ_{FR}	τ_{SR}	τ_c	τ_{FR}	τ_{SR}
15	74	52.4	2063	72	30.1	1536
20	4.5	7.2	513	24	5.1	508
25	1.01	0.89	115	0.31	1.8	189
30	0.22	0.05	89	0.06	0.07	190

Key: τ_c, relaxation time for collapse (h); τ_{FR}, relaxation time (h) for "fast" release; τ_{SR}, estimated relaxation time (h) for "slow" release.

reducing sugar in various inert matrices. Xylose and lysine were chosen because of their relatively high reactivity. They were incorporated in matrices having different characteristics, including simple sugars, polysaccharides, and other polymers. Samples were prepared from 20% solutions which were freeze dried and equilibrated to various moisture contents. Three types of experiments were done (Fig. 17): determination of the extent of browning at 20°C at various moisture contents (T = constant, T_g decreases with m, $(T - T_g)$ variable); determination of browning rates at different temperatures at a fixed moisture content (T variable, T_g fixed, $(T - T_g)$ variable); and determination of browning rates in systems where both temperature and moisture content were changed.

In systems in which crystallization occurs above T_g, e.g. trehalose sucrose, the crystallization may result in changes in reactant concentration in the solution phase. In the case of hydrate crystals, the reactants can be concentrated or diluted. In the case of anhydrous crystallization, the reactants are diluted in systems at constant a_w. The effects on reactivity can therefore be complex. Trehalose hydrate crystallization resulted in an increase in reaction rate.

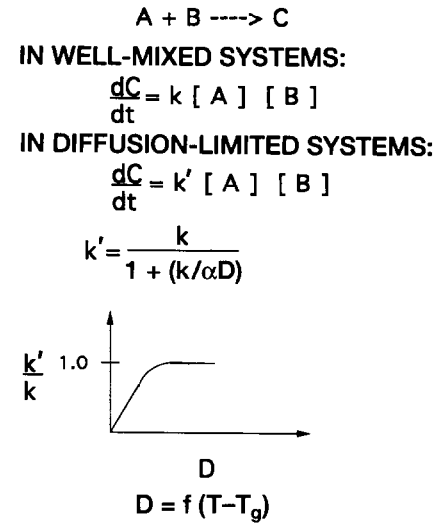

Fig. 16. Schematic representation of the effects of diffusional limitations in bimolecular reaction between reactants A and B to form C: k, reaction rate constant; k', apparent reaction rate constant in diffusion-limited systems; D, diffusivity of reactant; a, a constant.

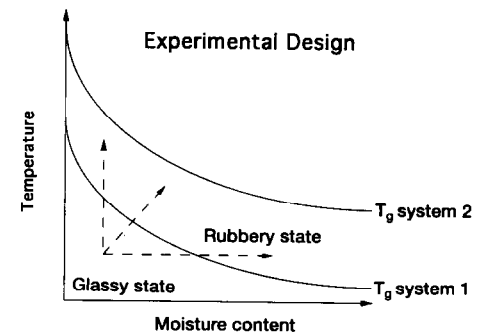

Fig. 17. Schematic representation of experimental design for studying reaction below and above T_g. Experiments for a given material can be done at various $(T - T_g)$ values by changing the temperature and/or moisture content. The system can also be changed.

In systems in which there is no crystallization, the situation is more complex. We studied xylose–lysine reactions in dry maltodextrins which do not crystallize. Two different maltodextrins of different molecular weights (MW 920 and MW 1200) were used. Solutions of a maltodextrin with xylose and lysine were prepared, put into vials, freeze dried, and dried over P_2O_5. The vials were then sealed and heated at various temperatures, after which browning was determined by optical density measurements at 420 nm. Arrhenius plots of zero-order browning-rate constants (Fig. 18) show the dependence of the rate of browning on temperature. The glass transition temperatures are indicated and identified by arrows. All experimental

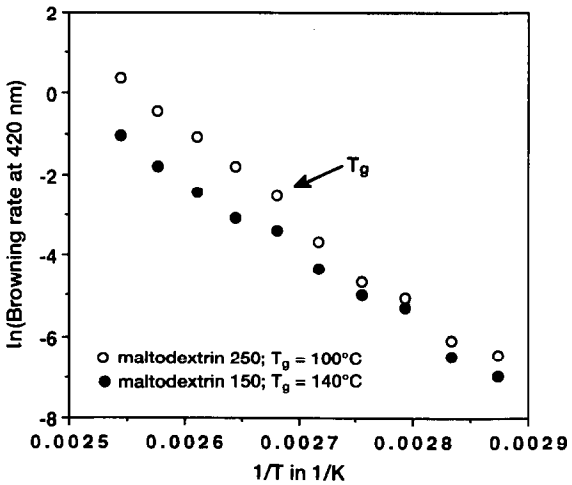

Fig. 18. Arrrhenius plots for browning reaction rates in two systems with different T_g values. Matrix : xylose : lysine = 94 : 5 : 1; $a_w = 0$.

temperatures were below the T_g for the MD (1200 MW) system while the experiments were conducted above and below the T_g for the MD 250 (900 MW) system. When the T_g of the maltodextrin 900 MW system is exceeded, the browning rates become noticeably faster than in the corresponding maltodextrin 1200 MW system. Below T_g, the browning rates are similar. The browning kinetic changes seem to occur in the vicinity of the T_g of the maltodextrin 900 MW system. Similar observations were made for the systems with other concentrations.

Browning results for PVP (MW = 10 000), xylose, and lysine (28 : 1 : 1) are shown in Fig. 19. In these experiments $(T - T_g)$ was changed by using different temperatures (changing T), as well as by having systems of different moisture contents (having different T_gs). Data are plotted as a function of $(T - T_g)$ with symbols representing samples of the same moisture content. Browning rates below T_g are low for all moisture contents. Above T_g, separate curves for browning at the different moisture contents are obtained. This indicates that effects of water and temperature are not fully explained by their impact on $(T - T_g)$. Similar results were seen for browning in PVP (MW = 40 000), xylose, and lysine samples, as well as in other systems. Statistical analysis has indicated that the variables temperature, moisture content, and glass transition are all important. However, adequate empirical models ($r^2 > 0.95$) can be obtained when browning rates are described by any 2 of the 3 terms: $(T - T_g)$, moisture content, or $1/T$(K).

A typical equation incorporating all 3 variables is shown below (obtained for polyvinylpyrrolidone : xylose : lysine (98 : 1 : 1)

$$\ln(k_B) = 18.42 - 7111\left(\frac{1}{T}\right) - 0.15m + 0.07(T - T_g)$$

where k_B is the browning rate constant in (OD units h^{-1}) and m is moisture in % (dry basis).

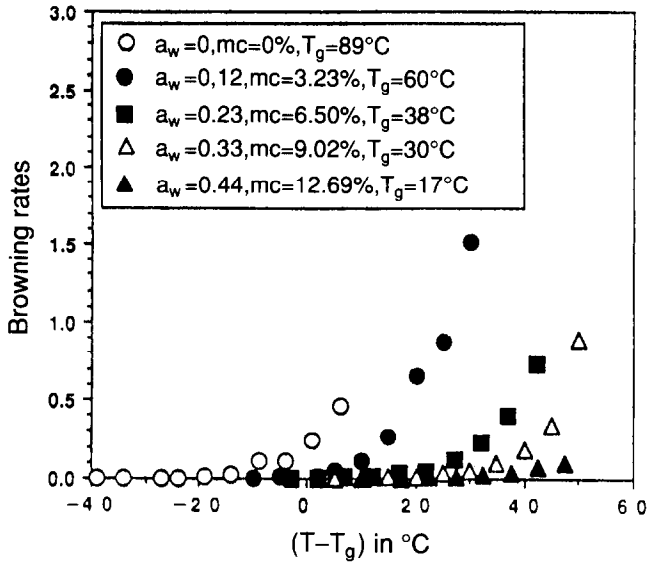

Fig. 19. Browning rates at various moisture contents and temperatures for the system polyvinylpyrrolidone:xylose:lysine (98:1:1).

9. Summary

The glass transitions of the amorphous components of foods affect the mobility of food components and this has drastic effects on food stability. The stability-related processes which were found to be affected by glass transition are: the stickiness and caking of powders, the crystallization of sugars and ice; the collapse of pores during dehydration, the diffusion of food components, and chemical reactions including non-enzymatic browning. Quantitative relations allowing the evaluation of the effects of the glass transition on food properties have been proposed.

Acknowledgments

This is publication No. D-10535-9-93 of the New Jersey Agricultural Experiment Station. Some of the work reported was supported by the State of New Jersey funds and the Center for Advanced Food Technology. The Center for Advanced Food Technology is a New Jersey Commission on Science and Technology Center.

References

[1] H.A.C. Thijssen and N.S.M. Van Oyen, Proc. 7th European Symposium, IUFoST, Eindhoven, The Netherlands, 1977, pp. 231–251.
[2] D.B. Lund, J. Food Process Preserv., 6 (1982) 133.

[3] T.P. Labuza and J.F. Kamman, in I. Saguy (Ed.), Computer-Aided Techniques in Food Technology, M. Dekker, New York, 1988, pp. 71–116.
[4] T.P. Labuza, S.R. Tannenbaum, and M. Karel, Food Technol., 24 (1970) 543–544, 546–548, 550.
[5] R. Heiss and K. Eichner, Haltbarmachen von Lebensmitteln, Springer, Berlin, 1990.
[6] O. Fennema, Food Chemistry, M. Dekker, New York, 1985, p. 56.
[7] M. Karel, Crit. Rev. Food Technol., 3 (1973) 329–373.
[8] M. Karel, in R. Duckworth (Ed.), Water Relations of Foods, Academic Press, London, 1975, pp. 435–463.
[9] G.W. Gould and J.H.B. Christian, in C.C. Seow (Ed.), Food Preservation by Moisture Control, Elsevier, London, 1988, pp. 43–56.
[10] G.S. Parks, H.M. Huffman and F.R. Caffoir, J. Phys. Chem., 32 (1928) 1366.
[11] H.C. Troy and P.F. Sharp, J. Dairy Sci., 13 (1930) 140.
[12] G.W. White and S.H. Cakebread, J. Food Technol., 1 (1966) 73–82.
[13] H. Levine and L. Slade, Comments Agric. Food Chem., 1 (1989) 315–396.
[14] L. Slade and H. Levine, Food Sci. and Nutrition, CRC Crit. Revs., 30(2,3) (1991) 115.
[15] M. Sugisaki, H. Suga and S. Seki, Bull. Chem. Soc. Jpn., 41 (1968) 2591–2599.
[16] G.P. Johari, A. Hallbrucker and E. Mayer, Nature, 330 (1987) 552–553.
[17] R.C. Hoseney, K. Zeleznak and C.S. Lai, J. Am. Assoc. Cereal Chem., 63(3) (1986) 285–286.
[18] Y. Roos and M. Karel, J. Food Sci., 56 (1991) 1676–1681.
[19] D. Simatos, M. Faure, E. Bonjour and M. Couach, Cryobiology, 12 (1975) 202–208.
[20] H. Levine and L. Slade, Carbohydr. Polym., 6 (1986) 213.
[21] Y.H. Roos, J. Food Sci., 52 (1987) 146.
[22] A.M. Cocero and J.L. Kokini, J. Rheol., 35(2) (1991) 257–270.
[23] Y. Roos and M. Karel, Cryo-Lett., 12 (1991) 367–376.
[24] E.M. de Graaf, H. Madeka, A.M. Cocero and J.L. Kokini, Biotechnol. Prog., 9 (1992) 210–213.
[25] M.T. Kalichevsky, E.M. Jaroszkiewica, S. Ablett, J.M.V. Blanshard and P.J. Lillford, Carbohydr. Polym., 18 (1992) 77–88.
[26] M. LeMeste, V.T. Huang, J. Panama, G. Anderson and R. Lentz, Cereal Foods World, 37 (1992) 264–267.
[27] Y. Roos and M. Karel, Biotechnol. Prog., 6 (1990) 159–163.
[28] T.J. Fox and P.J. Flory, J. Appl. Phys., 21 (1950) 581–591.
[29] Y. Roos and M. Karel, Biotechnol. Prog., 7 (1991) 49–53.
[30] M. Gordon and J.S. Taylor, J. Appl. Phys., 2 (1952) 493–500.
[31] Y.H. Roos, Carbohydr. Res., 238 (1993) 39–48.
[32] Y.H. Roos, J. Food Proc. Preserv., 16 (1993) 433–447.
[33] Y. Roos and M. Karel, Int. J. Food Sci. Technol., 26 (1991) 553–566.
[34] F. Franks, M.H. Asquith, C.C. Hammond, H.B. Skaer and P. Echlin, J. Microsc., 110 (1977) 223.
[35] Y. Roos and M. Karel, Food Technol., 45(12) (1991) 66–71, 107.
[36] M.L. Williams, R.F. Landel and J.D. Ferry, J. Am. Chem. Soc., 77 (1955) 3701.
[37] T. Soesanto and M.C. Williams, J. Phys. Chem., 85 (1981) 3338.
[38] M.E. Lazar, A.H. Brown, G.S. Smith and F.E. Lindquist, Food Technol., 10(3) (1956) 129–134.
[39] G.E. Downton, J.L. Flores-Luna and C.J. King, Ind. Eng. Chem. Fundam., 21 (1982) 447.
[40] B. Makower and W.B. Dye, J. Agric. Food Chem., 4 (1956) 72.
[41] Y. Roos and M. Karel, J. Food Sci., 57 (1992) 775–777.
[42] Y. Shimada, Y. Roos and M. Karel, J. Agric. Food Chem., 39 (1991) 637–641.
[43] K.J. Zeleznak and R.C. Hoseney, Cereal Chem., 64 (1987) 121–124.
[44] R.J. Bellows and C.J. King, Cryobiology, 9 (1972) 559.
[45] H. Levine and L. Slade, in J.R. Mitchell and J.M.V. Blanshard (Eds.), Food Structure—Its Creation and Evaluation, Butterworths, London, 1988, p. 149.
[46] M.J. Pikal and S. Shah, Int. J. Pharm., 62 (1990) 165–186.
[47] S.A. Anglea, V. Karathanos and M. Karel, Biotechnol. Prog., 9 (1993) 204–209.
[48] J.S. Vrentas and J.L. Duda, J. Appl. Polym. Phys., 22 (1978) 2325–2339.
[49] M. Karel in M.A. Rao and H. Schwartzberg (Eds.), Advances in Bio- and Food Engineering, M. Dekker, New York, 1990, pp. 277–294.

[50] J. Flink and M. Karel, J. Food Technol., 7 (1972) 199–211.
[51] E.C. To and J.M. Flink, J. Food Technol., 13 (1978) 583.
[52] S. Tsouroflis, J.M. Flink and M. Karel, J. Sci. Food Agric., 27 (1976) 509–519.
[53] M. Karel and I. Saguy, in H. Levine and L. Slade (Eds.), Water Relationship in Foods, Plenum Press, New York, 1992, pp. 157–173.
[54] M. Karel, in T. Richardson and J.W. Finley (Eds.), Chemical Changes in Food During Processing, AVI Publ. Co., Westport, CT, 1985, pp. 483–502.
[55] H. Levine, L. Slade, B. VanLengerich and J.G. Pickup, U.S. Patent 5,009,900, April 23, 1991.